

Computer Simulation on Terahertz Emission from Intrinsic Josephson Junctions of High- T_c Superconductors

Shizeng Lin^{1,3}, Xiao Hu¹ and Masashi Tachiki²

¹ National Institute for Materials Science, Tsukuba 305-0047, Japan

² Graduate School of Frontier Sciences, The University of Tokyo, Kashiwanoha 277-8568, Japan

³ Zhejiang Institute of Modern Physics, Zhejiang University, Hangzhou 310027, P.R. China

(Dated: May 21, 2007)

Solving coupled nonlinear sine-Gordon equations and Maxwell equations numerically, we study the electromagnetic and superconducting properties of the single crystal of high- T_c superconductor $\text{Bi}_2\text{Sr}_2\text{CaCu}_2\text{O}_{8+\delta}$ with a static magnetic field applied parallel to the ab -plane and a dc current fed in along the c -axis. Cavity resonances of transverse plasma occur in the intrinsic Josephson junctions with frequencies in terahertz regime. It is revealed that the electromagnetic wave can transmit from the junctions into space. The emitted energy counted by the Poynting vector is about $400\text{W}/\text{cm}^2$. The frequency as well as the energy of emission can be tuned almost continuously by the current and magnetic field.

PACS numbers: 74.50.74.25.Gz 85.25.Cp

Introduction – Terahertz (THz) technology is an extremely attractive field. The main users of the THz electromagnetic waves are perhaps the biomedical diagnostics, DNA probe and cancer detection; a THz tomography is also very useful for material characterization[1]. Although the lower and higher frequency bands of electromagnetic field can be generated by electronics and photonics respectively, seeking solid-state, stable generators for the THz waves is still a subject of scientific effort. While recently the semiconductor heterostructures generate THz emissions with high efficiency[2], known as the quantum cascade lasers, the issue of frequency tunability has not been resolved.

In the present work, following previous proposal[3], we seek continuously tunable emissions of THz electromagnetic waves from high- T_c superconductors with the principle of Josephson relation[4]. For this purpose, the highly anisotropic high- T_c superconductor $\text{Bi}_2\text{Sr}_2\text{CaCu}_2\text{O}_{8+\delta}$ can be considered as a stack of Josephson junctions in atomic scale[5]. The novel device has its advantages since, first, the energy gap in high- T_c superconductors is much larger than the plasma energy and thus the plasma, if excited in some way, should be stable; secondly, the power output conjectured to be proportional to the junction number squared would be very large; thirdly, variations of physical parameters in these intrinsic Josephson junctions (IJJs) are much smaller than artificially fabricated junctions. For artificial Josephson junction arrays, radiations of electromagnetic waves have been demonstrated[6]; the frequency is, however, in the sub-THz regime because of the small superconducting energy gap.

There are theoretical calculations[7] as well as numerical simulations[8, 9] which discussed possible radiation from IJJs of high- T_c cuprates. However, many issues have not yet been revealed concerning the mechanism of THz emission. Although the Josephson plasma ob-

viously play a key role here, the physical parameters of single Josephson junctions of $\text{Bi}_2\text{Sr}_2\text{CaCu}_2\text{O}_{8+\delta}$ only give plasma frequency in sub-THz regime. Therefore the collective modes in the stack of Josephson junctions are essential in order to lift the frequency by an order of magnitude. This goal is expected to be achieved by the Josephson vortices driven by the c -axis current, which generates oscillating voltage across junctions according to the ac Josephson relation. The Josephson plasma and the motion of vortices intervene with each other in a complex way, which makes the resonance condition in this system obscure. Without revealing the resonance mechanism, it is hard to tell whether a continuous tuning of frequency is possible or not.

On the other hand, experimental efforts toward exciting THz electromagnetic wave using IJJs seem to be accelerated recently [10, 11, 12]. However, there are large discrepancies in estimates of the optimal power output: theoretically $3000\text{W}/\text{cm}^2$ in Ref. [9], $1500\text{W}/\text{cm}^2$ in Ref. [7], while experimentally $150\text{W}/\text{cm}^2$ in Ref. [11], $20\text{W}/\text{cm}^2$ in Ref. [12], which hinders a clear assessment on the new technique.

In this paper, we investigate the THz radiation from intrinsic Josephson junctions by solving coupled nonlinear sine-Gordon equations numerically using an appropriate boundary condition. The main results of the present work are summarized as follows: Resonant radiation of THz wave occurs at the edge of junctions due to the cavity resonance of transverse plasma. A large resonance is achieved when the velocity of Josephson vortices matches the velocity of Josephson plasma. The vortex configuration is revealed to be rectangular with additional random sliding motions at resonance. The maximum energy is about $400\text{W}/\text{cm}^2$ and the frequency covers the THz band. Both the energy and frequency can be tuned almost continuously by the bias current and applied magnetic field.

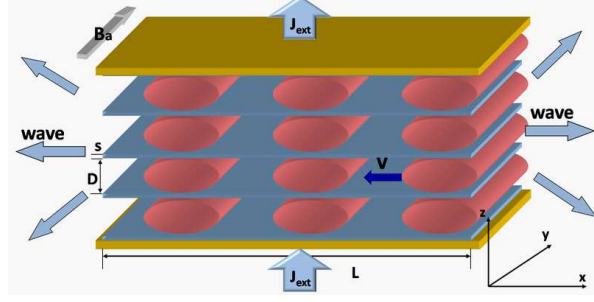


FIG. 1: (color online). Schematic diagram of terahertz electromagnetic wave emitter. The intrinsic Josephson junctions are sandwiched by two gold electrodes through which a dc bias current is fed into the system.

Model equations – The model we use, sketched schematically in Fig. 1 is the same as Ref.[9]. A static magnetic field B_a of order of 1T is applied along the y axis, which induces Josephson vortices in all insulating layers. A bias current is fed into the system along the z axis, which drives fluxons towards the negative direction of the x axis. The moving fluxons excite the transverse Josephson plasma[13, 14]. For simplicity, we ignore here the effect of thermal fluctuations and thus the vortex lines are straight. This approximation makes one to be able to reduce the three dimensional system to two dimensions. While the estimate on the output energy should be considered as the upper limit for experiments, the mechanism of radiation remains unchanged even when thermal fluctuations are involved.

Using the London theory, Josephson relation as well as Maxwell equations, the superconducting and electromagnetic properties of the system can be described by the following equations[9, 15, 16]:

$$(1 - \zeta \Delta^{(2)}) \{ \partial_{t'}^2 P_{l+1,l} + \beta \partial_{t'} P_{l+1,l} + \sin P_{l+1,l} + \alpha s' [\partial_{t'} (\rho'_{l+1} - \rho'_l) + \beta (\rho'_{l+1} - \rho'_l)] \} = \partial_{x'}^2 P_{l+1,l}, \quad (1)$$

$$s' (1 - \alpha \Delta^{(2)}) \rho'_l = \partial_{t'} (P_{l+1,l} - P_{l,l-1}), \quad (2)$$

where $P_{l+1,l}$ is the gauge invariant phase difference defined as

$$P_{l+1,l}(\mathbf{r}, t) = \varphi_{l+1}(\mathbf{r}, t) - \varphi_l(\mathbf{r}, t) - \frac{2\pi}{\phi_0} \int_{z_l}^{z_{l+1}} A_z(\mathbf{r}, t) dz, \quad (3)$$

with the phase of order parameter φ , the vector potential A_z and the quantum flux ϕ_0 . The operator $\Delta^{(2)}$ is defined as $\Delta^{(2)} f_l = f_{l+1} + f_{l-1} - 2f_l$. In Eqs.(1) and (2), dimensionless quantities are used: $x' = x/\lambda_c$, $t' = t\omega_p$ and $\rho'_l = \rho_l \lambda_c \omega_p / J_c$, where ρ_l is the charge density in the l th superconducting layer, $\omega_p = c/\lambda_c \sqrt{\epsilon_c}$ is the plasma frequency, ϵ_c is the dielectric constant along the z axis.

λ_c , and λ_{ab} in below, are the penetration depths. The other dimensionless quantities are defined as: $J' = J/J_c$, $B' = 2\pi\lambda_c DB/\phi_0$, $\beta = 4\pi\sigma_c \lambda_c / c \sqrt{\epsilon_c}$, $E' = \sigma_c E / \beta J_c$, $\alpha = \epsilon_c \mu^2 / sD$ (capacitive coupling), $\zeta = \lambda_{ab}^2 / sD$ (inductive coupling) and $s' = s/\lambda_c$, where σ_c is the conductivity, μ is the Debye screening length, J_c is the critical current density, s (D) is the thickness of the superconducting (insulating) layer.

Boundary condition – Equations (1) and (2) must be modified at the topmost and bottommost junctions. We assume that the superconductivity will penetrate into the gold electrodes[9] so that the thickness of the topmost and bottommost superconducting layers s_0 is larger than s . We also assume the electrodes as good conductor, therefore the electric field in the electrodes is zero. With these two assumptions, the equations at the topmost and bottommost layer can be written down straightforwardly[17].

The boundary condition at the edge ($x = 0$ and $x = L$) is more subtle. We implemented the dynamic boundary condition which is determined by the electromagnetic wave in the dielectric medium coupled to the junctions[7, 18]. Assuming that only transverse waves are transmitted through the dielectric medium, which becomes exact when the number of junctions is infinite, there is a linear relation between the electric and magnetic fields. With the Fresnel conditions, one arrives at following condition between the scillating fields \tilde{B}' and \tilde{E}' on the IJJs side of interface[18]

$$\tilde{B}'^y = \mp \sqrt{\epsilon'_d} \tilde{E}'^z, \quad (4)$$

where $+$ ($-$) means the wave propagating in the positive (negative) x direction, $\epsilon'_d \equiv \epsilon_d/\epsilon_c$ is the dielectric constant of the dielectric medium ϵ_d normalized by ϵ_c . With the relations $\partial_{x'} P_{l+1,l} = B'^y_{l+1,l}$ and $\partial_{t'} P_{l+1,l} = E'^z_{l+1,l}$, we derive from Eq.(4) the dynamic boundary condition for the IJJs

$$\partial_{x'} P_{l+1,l} - B'_a \pm \sqrt{\epsilon'_d} (\partial_{t'} P_{l+1,l} - E'_{dc}) = 0, \quad (5)$$

where the magnetic field induced by J'_{ext} is ignored because it is negligibly small in comparison to B'_a . In high-bias region $E'_{dc} \approx J'_{\text{ext}}/\beta$ (see [9]).

The parameters used for simulations are $\lambda_{ab} = 0.4\mu\text{m}$, $\lambda_c = 200\mu\text{m}$, $s = 3\text{\AA}$, $s_0 = 0.075\mu\text{m}$, $D = 12\text{\AA}$, $\mu = 0.6\text{\AA}$, $\alpha = 0.1$, $\beta = 0.02$ and $\epsilon_d = \epsilon_c = 10$. The number of junctions is $N = 30$ and the length is $L = 19.2\mu\text{m}$. The applied magnetic field is $B_a = 1\text{T}$. The equations of motion Eqs.(1) and (2) are integrated by the five-point Nordsieck-Gear Predictor-corrector method. The time step in all the simulations is set to $\Delta t' = 0.0002$ and the mesh size is set to $\Delta x' = 0.0002$ ($0.1\lambda_{ab}$). We start to calculate physical quantities when the system reaches steady states which are identified by the criterion that the voltage only fluctuates weakly around a fixed value.

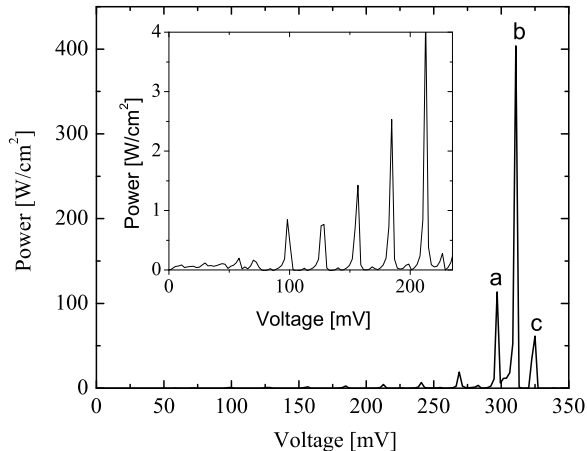


FIG. 2: Radiation power counted by the Poynting vector as a function of the voltage across the stack of IJJs. The external current corresponds to the b-peak is $J_{\text{ext}} = 1.33J_c$. The inset is the enlarged view of the main panel in the region $V < 235\text{mV}$.

Numerical results –We gradually ramp up the current J'_{ext} at $B_a = 1\text{T}$ and then gradually reduce it with step $\Delta J'_{\text{ext}} = 0.01$. The output power is counted by the Poynting vector at the left edge, toward which the vortices are moving. The dependence of power on voltage V is plotted in Fig. 2. The resonance takes place at discrete values of voltage with equidistance between neighboring peaks. The maximum power is about $400\text{W}/\text{cm}^2$.

The spectra of the electric field at the main peaks in Fig. 2 obtained by fast Fourier transformation are displayed in Fig. 3. The sharp spectra indicate monochromatic electromagnetic waves in *terahertz* regime. Thus we have confirmed theoretically the terahertz laser radiation from the intrinsic Josephson junctions.

The equidistance between neighboring peaks indicates a resonance phenomenon, the one between Josephson plasma and cavity modes as revealed below. The Josephson relation reads $\omega_{\text{JP}} = 2eV/\hbar$ and the cavity modes read $\omega_c = n\pi c_p/L$ where c_p is the velocity of transverse plasma and n is an integer. The resonance occurs when $\omega_{\text{JP}} = \omega_c$, namely

$$\bar{V} \equiv V/N = n\pi\hbar c_p/2eL. \quad (6)$$

To be more specific, we counted the wave length λ_w , frequency f and the voltage \bar{V} for the resonating peaks in Fig. 2; a-peak: $\lambda_w = 1.82\mu\text{m}$, $f = 4.79\text{THz}$, $\bar{V} = 9.90\text{mV}$; b-peak: $\lambda_w = 1.74\mu\text{m}$, $f = 5.01\text{THz}$, $\bar{V} = 10.36\text{mV}$ and c-peak: $\lambda_w = 1.66\mu\text{m}$, $f = 5.24\text{THz}$, $\bar{V} = 10.83\text{mV}$. It is easy to see that $f = 2e\bar{V}/\hbar$ and $n\lambda_w/2 = L$ for all the cases: a-peak, $n = 21$; b-peak, $n = 22$; c-peak, $n = 23$. The former is nothing but the Josephson relation and the latter is the condition for cav-

ity modes. From the wave length and the frequency, we estimate the plasma velocity as $c_p \approx 8.71 \times 10^6\text{m/s}$. It is then easy to see that the interval between consecutive peaks $\Delta\bar{V} = \pi\hbar c_p/2eL = 0.47\text{mV}$ is satisfied perfectly. Therefore our simulation indicates clearly that the terahertz laser is caused by the cavity resonance.

The above plasma velocities c_p is very close to the largest characteristic velocity $c_1 = 8.75 \times 10^6\text{m/s}$ obtained by solving the linearized Eqs.(1) and (2) with $s_0 > s$ (see also [19]). The velocity c_1 associated with the node-less mode is most important for resonance since it corresponds to the in-phase motion of vortices.

From Fig. 2, it is clear that there is a bundle of large resonances around $V = 310.8\text{mV}$ for $B_a = 1\text{T}$. In order to reveal the reason for this nonlinear property, we investigate the vortex motion. Since $P_{l+1,l} = 2\pi DB_a x/\phi_0 + 2\pi cDE_{l+1,l}^z t/\phi_0 + \tilde{P}_{l+1,l}$, where $\tilde{P}_{l+1,l}$ is the oscillating contribution, the velocity of vortices is evaluated as $v \approx cE_{l+1,l}^z/B_a = 8.63 \times 10^6\text{m/s}$ at the b-peak in Fig. 2. It is close to the plasma velocity c_p and c_1 . Therefore, the largest resonance takes place when the velocities of vortices and transverse plasma coincide with each other. A similar relation has been discussed in Ref. [20], where an infinitely long junction was considered and therefore no cavity mode was involved.

From $v = c_p = c_1$, it becomes clear that the largest energy emission is excited by a voltage

$$V = Nc_1 B_a D/c. \quad (7)$$

With Eqs. (6) and (7), we have $n = 2B_a LD/\phi_0$. Since $n\lambda_w/2 = L$, it is concluded that the optimal output is achieved when the wave length of plasma equals to the vortex-vortex separation $\lambda_w = \phi_0/B_a D$.

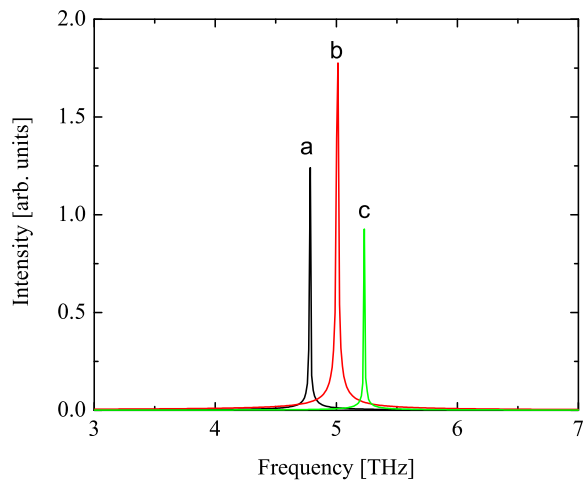


FIG. 3: (color online). Frequency spectra for the voltage at the main peaks in Fig. 2.

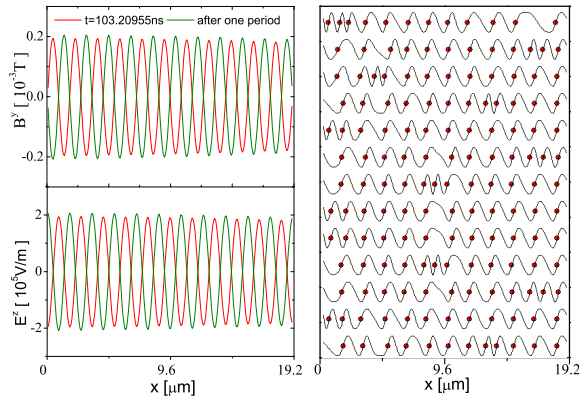


FIG. 4: (color online). Left panel: snapshots for the magnetic and electric fields at the largest resonance in Fig. 2, where the static backgrounds have been subtracted. Right panel: snapshot of vortex configuration.

It is interesting to take a look at the vortex configuration at resonance at this point. As seen from the snapshot shown in Fig. (4), the vortices form an overall ordered rectangular lattice; sliding motions take place in random places for the time being. The rectangular vortex lattice is in accordance with the matching between the measured electromagnetic wave velocity and the node-less plasma velocity.

Having clarified the mechanism of resonance, we turn to investigate how to tune the resonance frequency and

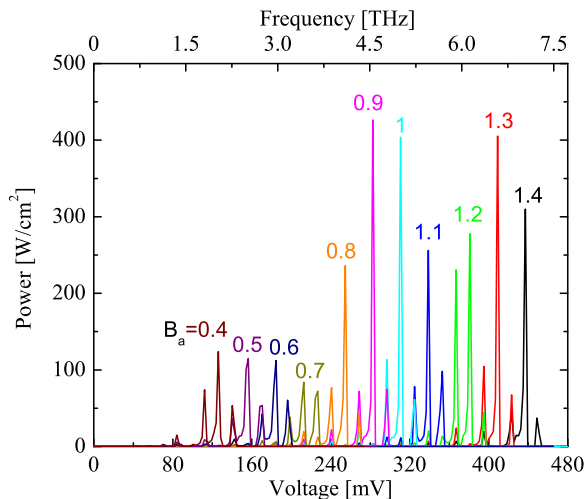


FIG. 5: (color online). Radiation power at different applied magnetic fields in units of Tesla as a function of the voltage across the stack of IJJs. The frequency in the upper axis is determined by the ac Josephson relation.

power. The voltage dependence of power emission at different magnetic fields is presented in Fig. 5. The voltage for largest power output increases linearly with the magnetic field, consistent with Eq. 7. From the ac Josephson relation, as depicted in the upper axis of Fig. 5, the frequency of emitted electromagnetic wave can be tuned by sweeping the magnetic field and adjusting the dc voltage accordingly. Although the cavity resonance imposes that the resonating frequency is discrete when voltage is swept, it becomes almost continuous if the length of IJJs L is large enough. For example, the frequency interval between neighboring resonances is about 0.04THz for $L = 100\mu\text{m}$.

At a given voltage, on the other hand, the emitted power shrinks quickly when the magnetic field is tuned away from the optimal matching value. This permits one to control the power output in a sensitive way.

Discussions – Finally we compare briefly our results with recent experimental works. Both Refs. [11] and [12] tried to stimulate THz electromagnetic waves utilizing the Josephson vortex dynamics. While the emission was detected by bolometer in Ref. [11], Ref. [12] used a second stack of IJJs to detect excited THz electromagnetic waves. It is somewhat difficult to draw conclusions on the resonance mechanism from experiments; in our simulation, however, cavity resonances are clearly observed. In Ref. [12] it is found that the most efficient emission is achieved for the rectangular vortex configuration, same as our computer simulation. Although not revealing a clear relation, both works tried to tune the frequency of emission by sweeping simultaneously the voltage and magnetic field, which, according to our theoretical investigation, is an efficient way for achieving the frequency tunability. In our simulation, we use magnetic fields below 1.5 Tesla, which are quite smaller than those in Ref. [12]. According to our relation for the optimal matching magnetic field and voltage, in order to get large emission power under 4 Tesla the voltage should be unrealistically large. It can be a possible reason that our theoretical estimate on the power output is different from that in the experiment.

Acknowledgements – X.H. acknowledges Q.-H. Chen and Y. Nonomura for discussions at the early stage of this study. Calculations were performed on SR11000 (HITACHI) in NIMS. X. H. is supported by Grant-in-Aid for Scientific Research (C) No. 18540360 and CTC program of JSPS, and project ITSNEM of China Academy of Science.

-
- [1] B. Ferguson and X.-C. Zhang, Nature Materials **1**, 26 (2002).
 - [2] R. Köhler, A. Tredicucci, F. Beltram, H. E. Beere, E. H.

- Linfield, A. G. Davies, D. A. Ritchie, R. C. Iotti and F. Rossi, *Nature*, **417**, 156 (2002).
- [3] T. Koyama and M. Tachiki, *Solid State Commun.* **96**, 367 (1995).
- [4] B. D. Josephson, *Phys. Lett.* **1**, 251 (1962); *Adv. Phys.* **14**, 419 (1965).
- [5] R. Kleiner, F. Steinmeyer, G. Kunkel and P. Müller, *Phys. Rev. Lett.* **68**, 2394 (1992).
- [6] P. Barbara, A. B. Cawthorne, S. V. Shitov and C. J. Lobb, *Phys. Rev. Lett.* **82**, 1963 (1999).
- [7] L. N. Bulaevskii and A. E. Koshelev, *J. Supercond. Nov. Magn.* **19**, 349 (2006).
- [8] M. Machida, T. Koyama and M. Tachiki, *Physica C* **362**, 16 (2001).
- [9] M. Tachiki, M. Iizuka, K. Minami, S. Tejima and H. Nakamura, *Phys. Rev. B* **71**, 134515 (2005).
- [10] I. E. Batov, X. Y. Jin, S. V. Shitov, Y. Koval, P. Müller and A. V. Ustinov, *Appl. Phys. Lett.* **88**, 262504 (2006).
- [11] K. Kadowaki, I. Kakeya, T. Yamamoto, T. Yamazaki, M. Kohri and Y. Kubo, *Physica C* **437**, 111 (2006).
- [12] M.-H. Bae, H.-J. Lee and J.-H. Choi, *Phys. Rev. Lett.* **98**, 027002 (2007).
- [13] K. Tamasaku, Y. Nakamura, and S. Uchida, *Phys. Rev. Lett.* **69**, 1455 (1992).
- [14] Y. Matsuda, M. B. Gaifullin, K. Kumagai, K. Kadowaki and T. Mochiku, *Phys. Rev. Lett.* **75**, 4512 (1995).
- [15] S. Sakai, P. Bodin and N. F. Pedersen, *J. Appl. Phys.* **73**, 2411 (1993).
- [16] M. Machida, T. Koyama, and M. Tachiki, *Phys. Rev. Lett.* **83**, 4618 (1999).
- [17] T. Koyama and M. Tachiki, *Phys. Rev. B* **54**, 16183 (1996).
- [18] L. N. Bulaevskii and A. E. Koshelev, *Phys. Rev. Lett.* **97**, 267001 (2006).
- [19] S. Sakai, A. V. Ustinov, H. Kohlstedt, A. Petraglia and N. F. Pedersen, *Phys. Rev. B* **50**, 12905 (1994).
- [20] A. E. Koshelev and I. S. Aranson, *Phys. Rev. Lett.* **85**, 3938 (2000); *ibid* *Phys. Rev. B* **64**, 174508 (2001).